



DIGITAL ACCESS TO
SCHOLARSHIP AT HARVARD
DASH.HARVARD.EDU



HARVARD LIBRARY
Office for Scholarly Communication

A bottom-up perspective on ecosystem change in Mesozoic oceans

The Harvard community has made this article openly available. [Please share](#) how this access benefits you. Your story matters

Citation	Knoll, Andrew H., and Michael J. Follows. 2016. "A bottom-up perspective on ecosystem change in Mesozoic oceans." <i>Proceedings of the Royal Society B: Biological Sciences</i> 283 (1841): 20161755. doi:10.1098/rspb.2016.1755. http://dx.doi.org/10.1098/rspb.2016.1755 .
Published Version	doi:10.1098/rspb.2016.1755
Citable link	http://nrs.harvard.edu/urn-3:HUL.InstRepos:29626183
Terms of Use	This article was downloaded from Harvard University's DASH repository, and is made available under the terms and conditions applicable to Other Posted Material, as set forth at http://nrs.harvard.edu/urn-3:HUL.InstRepos:dash.current.terms-of-use#LAA



Cite this article: Knoll AH, Follows MJ. 2016
A bottom-up perspective on ecosystem change
in Mesozoic oceans. *Proc. R. Soc. B* **283**:
20161755.
<http://dx.doi.org/10.1098/rspb.2016.1755>

Received: 8 August 2016

Accepted: 20 September 2016

Subject Areas:

palaeontology

Keywords:

phytoplankton, ecosystem model, predation

Author for correspondence:

Andrew H. Knoll

e-mail: aknoll@oeb.harvard.edu

A bottom-up perspective on ecosystem change in Mesozoic oceans

Andrew H. Knoll¹ and Michael J. Follows²

¹Department of Organismic and Evolutionary Biology, Harvard University, Cambridge, MA 02138, USA

²Department of Earth, Atmospheric and Planetary Sciences, Massachusetts Institute of Technology, Cambridge, MA 02139, USA

AHK, 0000-0003-1308-8585

Mesozoic and Early Cenozoic marine animals across multiple phyla record secular trends in morphology, environmental distribution, and inferred behaviour that are parsimoniously explained in terms of increased selection pressure from durophagous predators. Another systemic change in Mesozoic marine ecosystems, less widely appreciated than the first, may help to explain the observed animal record. Fossils, biomarker molecules, and molecular clocks indicate a major shift in phytoplankton composition, as mixotrophic dinoflagellates, coccolithophorids and, later, diatoms radiated across shelves. Models originally developed to probe the ecology and biogeography of modern phytoplankton enable us to evaluate the ecosystem consequences of these phytoplankton radiations. In particular, our models suggest that the radiation of mixotrophic dinoflagellates and the subsequent diversification of marine diatoms would have accelerated the transfer of primary production upward into larger size classes and higher trophic levels. Thus, phytoplankton evolution provides a mechanism capable of facilitating the observed evolutionary shift in Mesozoic marine animals.

1. Introduction

In 1977, Geerat Vermeij [1] documented a pattern of widespread and persistent evolutionary change among benthic invertebrates in Mesozoic (252–66 Ma) oceans, a transformation he christened the Mesozoic marine revolution and interpreted in terms of increasing selection pressure by durophagous predators. This explanation suggests classic top-down control of ecosystem composition, but Vermeij recognized that the most straightforward way to increase predator abundance would be to boost primary production, adding a critical bottom-up component to his argument (later expanded and formalized as the theory of escalation [2,3]). Estimating the productivity of ancient oceans is challenging [4,5], with some of the most compelling, if indirect, arguments for secular increase in primary production coming from patterns of marine animal diversity, the very thing one would like to explain [6,7]. Here, we take a complementary approach and ask how animals in marine ecosystems would be affected by a change in the *composition* of primary producer communities. Our thesis is that observed Mesozoic changes in the composition of continental shelf phytoplankton can indeed help us to understand Mesozoic marine animal evolution.

2. Patterns of animal evolution in Mesozoic oceans

Vermeij [1] insightfully applied ecological variations detected in space to illuminate evolutionary patterns observed through time. Specifically, he noted that the claws of predatory crabs in the tropical Indo-Pacific region have greater crushing strength than those in the Western Atlantic Ocean; concomitantly, Indo-Pacific gastropods have thicker shells, more prominent defensive ornamentation, and coiling patterns better able to withstand compressive forces [8]. Indeed, Vermeij

[9] argued more generally that spatial variations in the abundance and armament of shell-crushing predators covary with patterns of skeletal morphology in prey organisms.

Vermeij's arguments about Mesozoic marine evolution focused, in the first instance, on the gastropods so central to his ecological observations. Planispiral and open-coiled shells are common in upper Paleozoic and Triassic rocks; most have wide apertures and minimal ornamentation. Beginning in the Jurassic, however, such forms were increasingly supplanted by taxa with coiling more resistant to crushing, narrower and sometimes toothed apertures, and prominent spines and other ornaments—all recognized as morphological ways to avoid or survive durophagous predation. Underpinning the evolution of spines was the physiological ability to resorb and remodel shell carbonate during growth, a capacity widespread in younger but not older gastropods [1]. Continuing ecological research has strengthened the view that in modern oceans gastropod shell form varies as a function of predator pressure (e.g. [10–13]).

Other molluscs show comparable evidence for increased predation in Mesozoic oceans. Ammonites, for example, record an increasing incidence of shell repair in younger Mesozoic rocks [14,15], and ecological research confirms that shell repair structures faithfully record predator pressure [16]. Bivalves commonly escape predators by living infaunally. While bivalves evolved the ability to burrow early in their evolutionary history [17], most Paleozoic taxa were epifaunal or semi-infaunal [18]. Triassic and Lower Jurassic rocks are full of epifaunal bivalves, especially oysters and their relatives, but later in the Jurassic and continuing into the Cenozoic, bivalve assemblages increasingly became dominated by infauna, with epifaunal bivalves either motile (which facilitates predator avoidance [19]) or, save for the massively calcified rudists, limited to habitats where salinity or physical parameters inhibit predator populations [18,20–22].

Echinoderms also show both morphological and ecological responses to increasing predation. Stalked crinoids, ecologically important components of Paleozoic shelf and platform faunas, increasingly became limited to deeper habitats where predation is less common [23]; at the same time, crinoids in shallow marine environments increasingly evolved motility [24,25]. Brittle stars also became less abundant in shallow water environments, at least partly because of increased predator pressure [26,27]. Through the Mesozoic Era, skeletons of epifaunal echinoids exhibited both increasing mechanical strength and more conspicuous defences, especially spines, while infaunal echinoids radiated across shelves [28]. Once again, there is evidence for increased predation on crinoids within Triassic oceans [24], but this does not obviate the sweep of morphological and behavioural shifts observed from the Jurassic onward. Brachiopods also evolved increasing ornamentation in earlier Mesozoic oceans, but because options for defence enhancement were limited, most clades eventually declined in abundance and diversity [29,30]. Even calcifying red algae changed morphologically in the face of increased grazing by durophagous herbivores [31].

It is worth noting criticism of the Vermeij hypothesis, particularly a statistical analysis of diversity dynamics by Madin *et al.* [32], whose analysis recovered secular changes in diversity among infauna, motile epifauna, sessile epifauna, and carnivores consistent with those expected by Vermeij, but who argued for the statistical independence of these patterns. Rebuttals ([33–35], but see also [36]) have challenged the taxonomic,

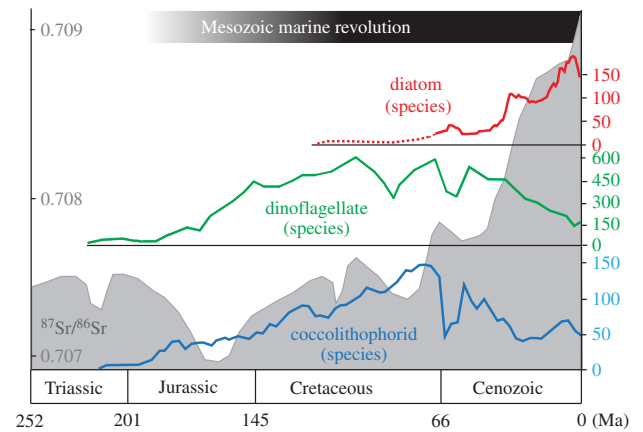


Figure 1. The Mesozoic marine revolution occurred during an extended interval of significant evolutionary change in marine primary producers, including radiations of photosynthetic dinoflagellates (green), coccolithophorids (blue) and, subsequently, diatoms (red). Strontium (Sr) isotopes (grey) suggest a significant enhancement of weathering and nutrient enrichment of the global ocean on the same time scale as (potentially related) diatom diversification. Microfossil diversity replotted from Falkowski *et al.* [48], based on original tabulations from Spencer-Cervato [49], Bown *et al.* [50], and Stover *et al.* [51]; strontium isotope data from Veizer *et al.* [81].

temporal, and spatial scales of this criticism, a key point being that broad scale diversity trends shed limited light on hypotheses about specific morphological features and behaviour.

In general, then, a persistent pattern of evolution characterizes skeletal organisms across several phyla in Mesozoic continental platform and shelf environments, and as Vermeij ([1], see also [37]) proposed, this pattern is parsimoniously explained by an increase in the abundance, size, and/or armament of the animals that preyed on these organisms. Fossils provide direct support for a Mesozoic–Cenozoic radiation of durophagous predators. Durophagy evolved long before the Mesozoic marine revolution (e.g. [38]) but shell-crushing fish [1], tetrapods [39], crustaceans [40], and predatory gastropods [41], asteroids [42], and echinoids [25] all show evidence of later Mesozoic and Cenozoic diversification. More generally, the proportional diversity of predators in among marine fossils has increased through the past 150 Myr [43,44], as have both the incidence of drill holes and repair scars on fossil skeletons [45] and crushed shell debris [46].

3. A second Mesozoic marine revolution

Today, diatoms, dinoflagellates, and coccolithophorids dominate primary production in continental shelf waters, and these are also the most abundant and diverse eukaryotic phytoplankton in the blue-water oceans [47]. All rose to ecological prominence in Mesozoic oceans and none is reliably recorded from earlier seas, where cyanobacteria and green phytoflagellates appear to have predominated ([48]; figure 1). This phytoplankton makeover is recorded by the biomineralized skeletons of diatoms and coccolithophoroids and by organic-walled dinoflagellate cysts. These records are potentially subject to preservational bias through time—one might imagine, for example, that early diatoms were only weakly mineralized, or that early dinoflagellates did not form recognizable cysts, obscuring an evolutionary history far longer than that recorded by microfossils. Steranes and other molecular biomarkers, however, provide a second record of

phytoplankton evolution that largely corroborates the one reconstructed from microfossils [53–55], suggesting that marine sediments faithfully record a Mesozoic revolution in phytoplankton composition. Neither do molecular clocks suggest long prehistories for these clades [56–59]. Unambiguous dinoflagellate microfossils first appear in upper Triassic rocks and the group radiated through the Jurassic, reaching a diversity maximum in Cretaceous oceans, and much the same is true of coccolithophorids [60]. Diatoms diversified later, during the Late Cretaceous and, especially, Cenozoic [49,61–63].

Radiating Mesozoic clades differ from Paleozoic phytoplankton dominants in a number of traits. Dinoflagellates and diatoms commonly have larger cells than those of Paleozoic cyanobacteria and green algae. Diatoms and coccolithophorids are armoured, and, importantly, dinoflagellates are commonly mixotrophic. How might observed changes in the phytoplankton have influenced the faunal events identified by Vermeij?

4. A trait-based perspective on phytoplankton evolution

Current theoretical and modelling understanding of the functional and taxonomic biogeography of marine phytoplankton focuses on traits and trade-offs. Understanding and quantifying the key costs and benefits of a particular trait allows us to build diagnostic and predictive models. As an example, nitrogen (N) fixation relieves nitrogen stress in certain environments but has a high energetic cost, largely associated with oxygen management to protect nitrogenase; this cost reduces growth rates and growth efficiencies [64,65]. In addition, nitrogen fixers have a high iron demand to maintain the required nitrogenase [66]. With this understanding, using resource ratio theory, we can predict and interpret the biogeography of nitrogen fixation observed in today's oceans [67].

Key traits in any ecosystem include maximum growth rates, resource affinities, and defence characteristics. In a simplified model, consider the rate of change of biomass of phytoplankton phenotype i (B_i , mol kg⁻¹):

$$\frac{dB_i}{dt} = \mu_{o,i} \frac{R}{R + K_i} B_i - m_i B_i. \quad (4.1)$$

We assume that Monod-kinetics appropriately describe resource-dependent growth, where R (mol l⁻¹) is the limiting resource, $\mu_{o,i}$ (s⁻¹) is the maximum growth rate, and K_i (mol l⁻¹) is the half-saturation. m_i (s⁻¹) represents all loss processes as a simple fixed rate. Two interesting limits reveal the significance of these traits for fitness. In a situation where resources are replete, net *per capita* rate of population increase depends on maximum growth and loss rates:

$$\frac{1}{B_i} \frac{dB_i}{dt} = \mu_{o,i} - m_i. \quad (4.2)$$

Resource replete conditions are almost always intermittent and in such situations, over several cycles of replenishment, selection will favour the highest *per capita* growth rate that can be achieved by high maximum growth rate or good defence against losses. By contrast, in a steady state where nutrients are consistently depleted, the solution of (4.1) predicts that the subsistence resource concentration of phenotype i will be defined by its traits as follows:

$$R_i^* = \frac{K_i m_i}{\mu_{o,i} - m_i}. \quad (4.3)$$

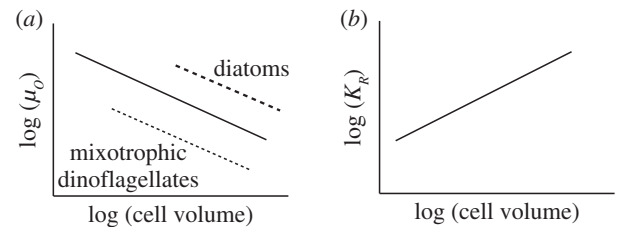


Figure 2. Schematic view of the power law relationships between cell volume and key traits of marine phytoplankton. These relationships are rooted in empirical observations and understood in terms of geometric effects on resource acquisition. (a) Maximum growth rate versus cell volume. The solid black line indicates the general trend used in the control model. Mixotrophic dinoflagellates (dotted line) follow the same trend but trade-off a lower growth rate against a generalist resource acquisition strategy. Diatoms (dashed line) are capable of faster maximum growth rates than other phytoplankton. (b) Resource half-saturation for the Monod-kinetics growth model versus cell volume.

The competitive exclusion principle suggests that, at equilibrium, the population with the lowest R^* will exclude all others that are limited by the same resource [68,69]. Hence, maximum growth rate and mortality (defence) are key traits in both resource replete and oligotrophic conditions. Resource affinity (and K_i) is also significant in the latter case.

How were these traits affected by the Mesozoic innovations among primary producers, and how would this have affected the structure of marine communities? Could these innovations have stimulated from the bottom-up some of the changes observed at higher trophic levels? To address these questions, we first discuss the allometric and functional structuring of key traits and then construct a simple numerical model of plankton population structure and productivity with which to explore several hypotheses.

(a) Allometric constraints on productivity

Numerous studies have empirically demonstrated the scaling of reproductive rate with body size, showing a negative power law relationship from unicellular protists all the way to large mammals and trees. In eukaryotic phytoplankton, maximum growth rate ($\mu_{o,i}$, d⁻¹) and cell volume V_i (μm^3), follow the relationship $\mu_{o,i} = 0.7V_i^{-0.24}$ d⁻¹ [70]: larger organisms have slower maximum growth rates. By contrast, nutrient half-saturation increases with cell volume: $K_i = 0.17V_i^{0.27}$ $\mu\text{mol N l}^{-1}$ for nitrate-limited growth (figure 2).

Larger cells have both slower maximum growth rates and higher R^* s. Thus, from a growth perspective, smaller cells should outcompete them everywhere. Indeed, the smallest primary producers are specialist gleaners that dominate the most oligotrophic marine environments. However, top-down control prevents them from sequestering all of an available resource, enabling populations of larger cells to coexist with grazer-controlled smaller cells [71–73]. If the maximum population size of primary producers is controlled by grazing (or viral losses), then, as the rate of resource supply increases, so too will the body size of the largest cells that can be supported.

This can be illustrated by extending the model above to include prey-specific predators and an explicit mass balance for the resource (described in box 1).

Here we use a highly idealized model of the planktonic food web, depicted schematically in figure 3, to illustrate how size-dependent traits shape both the pattern of

Box 1. A simplified ecosystem model with allometric constraints on traits.

In equation (4.4), we define the governing equation for the rate of change of biomass of plankton type i (B_i , mol m⁻³). Growth is represented by Monod-kinetics, limited by a single resource R (mol l⁻¹), with maximum growth rate μ_{oi} (s⁻¹), and resource half-saturation K_i (mol l⁻¹). Cells can consume, and be consumed, by an arbitrary combination of the other plankton types (second and third terms on the right, respectively), both described as Holling II functional response models. Predatory gains are governed by a matrix of maximum growth rates, g_{oji} ((mol l⁻¹ s⁻¹), where ji refers to type j consuming type i . Maximum grazing rates are set by the empirically informed, allometric power law: $g_{oji} = 3.3V_i^{-0.16}$ ((mol l⁻¹ s⁻¹) ([74], with assumptions as in [73]). Predatory losses are described similarly. γ_{ji} is the efficiency with which consumed prey is converted to predator biomass. Finally, the fourth term on the right of (4.4) represents losses due to maintenance respiration and other, non-specific mortality. Equation (4.5) describes the community consumption of the inorganic resource, R , and its resupply, S_R .

$$\frac{dB_i}{dt} = \mu_{oi} \frac{R}{R + K_i} B_i + \sum_{j=1}^n \gamma_{ji} g_{oji} \frac{B_j}{B_j + k_{Bji}} B_i - \sum_{k=1}^n g_{oik} \frac{B_i}{B_i + k_{Bik}} B_k - m_i B_i \quad (4.4)$$

and

$$\frac{dR}{dt} = - \sum_{i=1}^n \mu_{oi} \frac{R}{R + k_{Ri}} B_i + S_R. \quad (4.5)$$

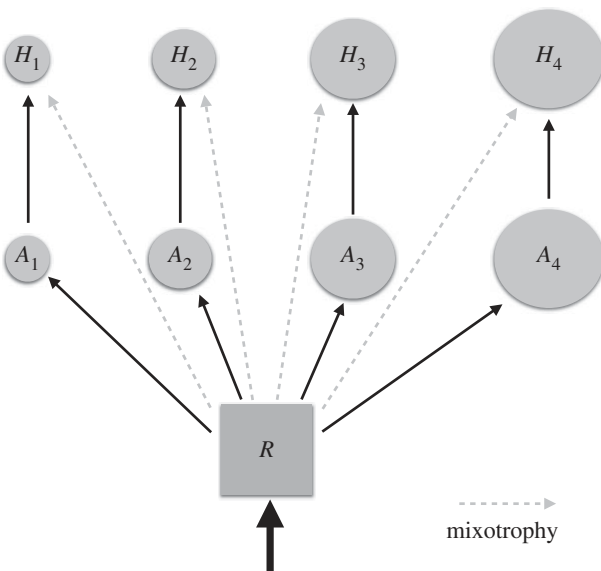


Figure 3. Schematic depiction of the simplified model employed here. A single inorganic resource, R , sustains an assemblage of photoautotrophs (A_i) each of which is consumed by a specific predator (H_i). Cell volume/body size increases with index i . Solid black lines indicate the flow of resource in the purely specialist (autotroph/heterotroph) model. Dashed grey lines indicate the additional flows when mixotrophy is introduced into the model.

phytoplankton assemblages and the delivery of organic carbon to larger size classes. The model resolves four size classes of photoautotroph and four associated size classes of predatory heterotrophs. The mathematical framework is as described in box 1 and the traits (maximum growth and grazing rates, resource half saturations) are governed by the empirical power law relationships discussed above. The set of ordinary differential equations was integrated forward in time from an arbitrary initial condition to steady state for a range of rates of supply of the inorganic resource. As shown in figure 4, as resource supply increases so too does the capacity for larger primary producers and their predators to coexist with the smaller types. In figure 4, the lowermost solid line indicates the biomass of the smallest size class of primary producer as a function of nutrient supply. The next line indicates the cumulative biomass of the two smallest

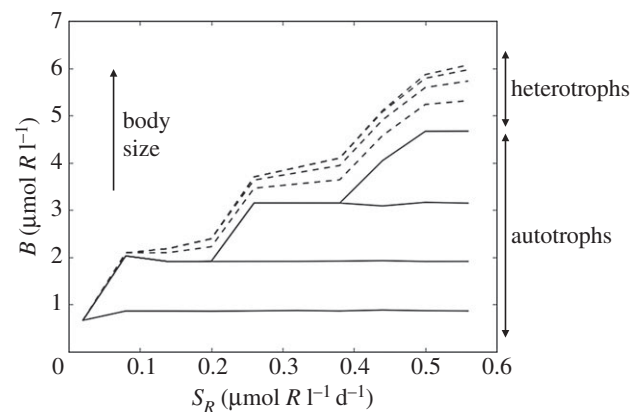


Figure 4. Cumulative biomass (B) with size as a function of resource supply rate (S_R) in the 'control' model where maximum growth rate strictly follows the solid black line in figure 2a. The uppermost dashed line indicates total plankton biomass, summing the contributions from each size class of both autotrophs (solid lines) and heterotrophs (dashed lines) which are stacked with contributions from the smallest autotrophs at the bottom, and heterotrophs on top of autotrophs.

size classes and so on. Dashed lines indicate the contribution to total biomass from the associated predators in a similar way, and so the uppermost dashed line reflects the total standing biomass in the system as a function of the rate of delivery of inorganic resource. At the lowest resource supply rates, only the smallest phytoplankton classes are viable; they have the lowest R^* and outcompete the larger cells but their own population remains too small to sustain a predator. However, as the nutrient supply increases so too does their population size until it reaches the subsistence level for their predators. This top-down control prevents further increase in the population size of the smallest autotrophs and caps their rate of resource consumption so that at even higher resource supply rates, some resource is available to larger size classes, which grow in until they also become subject to predation, and so on. This stacked relationship among size classes in the plankton is observed in the ocean today (e.g. [73,75]), providing empirical support for the mechanistic model. The simple framework can be adapted to represent more complex food webs with richer

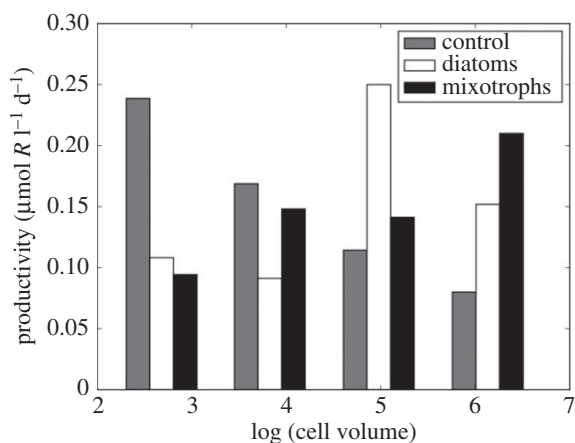


Figure 5. Total system productivity (primary and secondary) as a function of size class in the model at the highest resource supply rate shown in figure 4. Grey bars indicate the control solution where maximum growth rate strictly follows the solid black line in figure 2*a*. White and black bars indicate the model into which diatoms and mixotrophy were introduced, respectively, as described in the text.

interaction networks, but they retain the same qualitative structure and implications [67,71].

The size distribution of biomass is rather flat (not illustrated), due to the top-down control by grazing, consistent with observed size spectra [76]. Here, however, we are concerned with the flow of material and energy up to the larger organisms that ultimately depend on these primary producers. The grey bars in figure 5 illustrate total productivity (autotrophic and heterotrophic; $\text{mol l}^{-1} \text{d}^{-1}$) in each size class of the model at the highest nutrient supply rate shown in figure 4 where all four size classes coexist. Trophic transfer efficiency is low (here assumed to be 10%), and so in this ‘control’ model, where the traits exactly follow the allometric scalings, total productivity declines rapidly with increasing size. Since predatory plankton tend to consume organisms about an order of magnitude smaller than themselves [74], the biomass and productivity of the smallest cells is not directly accessible to large predators. The rapid decline in productivity with size means that the upwards flow of resources is relatively small, limiting productivity and population size higher up the food chain.

Hence, in a system where allometric constraints on resource affinities entirely dictate the assemblage, the delivery of material to larger size classes and higher trophic levels is very low. However, modification of the allometric relationships by alternative trophic strategies and physiological innovations can relieve this constraint. We illustrate two such mechanisms in the context of the model below.

(b) Mixotrophy

Evolutionary innovations have modified the traits of primary producers, fuelling greater productivity in larger size classes which, we hypothesize, contributed a bottom-up stimulus for Mesozoic animal evolution. Not all phytoplankton lie on the same size-growth rate relationship (solid line in figure 2*a*). Notably, mixotrophic dinoflagellates trade-off the benefits of a generalist (autotrophic and phagotrophic) approach to nutrition against a slower maximum growth rate, size for size, relative to pure autotrophs (figure 2*a*, dashed line; see [77]). As large cells with inefficient resource acquisition and, hence,

low growth rates, dinoflagellates would appear to compete poorly against other phytoplankters; however, because they can gain nutrients by phagocytosing other cells, mixotrophic dinoflagellates are both abundant and diverse in contemporary oceans. That is, mixotrophy allows larger cells to supplement resources for which they are less competitive (i.e. have higher R^*) with respect to the inorganic form. This enables primary production of new organic material in larger size classes and enhances the flow of organic resources to higher trophic levels [78]. In a simple demonstration of this effect, we introduced mixotrophy into our model by allowing the heterotrophs to also grow autotrophically (i.e. assume a mixotrophic lifestyle) but with much reduced uptake rates (approx. 55%) for inorganic resources relative to the specialists. In figure 5, the black bars illustrate the resulting size structuring of productivity: the introduction of mixotrophy leads to a significant enhancement of productivity in the largest size classes, relative to the control case. In this highly simplified model, total productivity is greater in the larger size classes when mixotrophy is active. The general principle is borne out in more complex global ocean ecosystem simulations [74]. Hence, the radiation of mixotrophic dinoflagellates may have significantly altered the structure of marine productivity, providing bottom-up fuel for the Mesozoic marine revolution (figure 1).

(c) Diatoms

Later on (figure 1), the diversification of marine diatoms opened up a new niche for highly effective opportunists. Size for size, diatoms have higher maximum growth rates than other phytoplankton, possibly related to the cost-effectiveness of building a silica-based frustule [79]. The frustules also provide effective defence. Hence, diatoms innovated both an enhancement to μ_0 and a reduction in m , improving their relative fitness both in boom-bust and stable, oligotrophic environments. In a further sensitivity study with the model, we examined the impact of enhancing the maximum growth rate of the two largest size classes (dashed line, figure 2*a*), mimicking the evolution of large, fast-growing diatoms (now in the absence of mixotrophy). The impact on the size dependence of productivity is shown in figure 5 (white bars). Higher growth rates provide an advantage for the diatoms, increasing total productivity in the larger sizes and the rate at which resources can be delivered to even larger (but unresolved) size classes and higher trophic levels.

5. Discussion

Our simple model illustrates three key concepts relevant to the Mesozoic marine revolution. Firstly, the model shows that the Mesozoic radiation of mixotrophic dinoflagellates would have enhanced the flow of resources to larger size classes and higher trophic levels (figure 5). Secondly, any increase in the rate of nutrient supply to the surface ocean would have opened a niche for larger primary producers (figure 4); packaging phytoplankton into larger cells will shorten food chains at the lower end, again enhancing upwards resource flow. And thirdly, the opening of that niche may have facilitated the rise of large, silicified diatoms, whose adaptation for fast growth rates in replete environments would have further accelerated the enrichment of higher trophic levels (figure 5). Thus, these interconnected events could underpin the evolutionary trajectories observed among marine metazoan fossils.

A predicted result of dinoflagellate radiation is the shortening of food chains, delivering more energy and biomass to the predatory populations at the apices of food webs [78]. Even in small amounts, mixotrophy should enhance community productivity [52]. We suggest that this enhancement of resource delivery to larger size classes and higher trophic levels contributed a bottom-up push to the Mesozoic marine revolution, providing fuel for the ensuing arms race between the consumers of primary producers and their predators.

Our current understanding of the size structuring of plankton biomass makes a clear case that larger size classes, with low nutrient affinities, are largely excluded from regions of low nutrient supply. Conversely, enhanced nutrient supply fuels a growing in of larger organisms (e.g. figure 4). Could a global-scale enrichment of ocean nutrients have driven a parallel restructuring of phytoplankton on a similar scale? As noted above, quantitative estimates of ancient primary production are hard to come by, and existing geochemical proxies commonly target export production, which has a complicated relationship to primary production in surface waters [4,80]. To the extent that nutrient fluxes from continental weathering and erosion regulate primary production in the oceans, one might assume that geochemical proxies for run-off should provide at least a qualitative indication of changing primary production through time. Thus, increasing $^{87}\text{Sr}/^{86}\text{Sr}$, an indication of increasing continental input of Sr to seawater, relative to hydrothermal sources, should correlate with increasing phosphorous (P) fluxes into the ocean. A well-resolved record of seawater strontium isotopes has been constructed from analyses of skeletal carbonates [81]; this record suggests that primary production might well have increased nearly monotonically from the later Cretaceous Period to the Neogene, concomitant with the rise of diatoms to ecological prominence. Long-term secular trends are less obvious in earlier Mesozoic oceans; $^{87}\text{Sr}/^{86}\text{Sr}$ values do not exceed Triassic to earliest Jurassic maxima until the end of the Cretaceous Period (figure 1). Seawater strontium isotopes reflect the lithologies of eroding continental rocks as well as the amount of run-off, complicating attempts to quantify erosional fluxes [82]. Nonetheless, sediment accumulation rates [83] and thermochronology [84] both reinforce the view that erosional fluxes in the oceans increased through the Cenozoic Era. Lithium (Li) isotopes have more recently been applied to questions of continental weathering, and these also corroborate the hypothesis of increased weathering fluxes through the Cenozoic Era, reaching a high steady state over the past 10 Myr [85,86]. Limited Li isotopic data are also consistent with lower weathering fluxes before the latest Cretaceous Period (e.g. [87]). Proxies for continental weathering and erosion are, thus, consistent with the hypothesis of increasing resource availability at the base of marine trophic pyramids over the last 80 Myr or so, helping to explain the persistence if not the initiation of predator-driven evolutionary trends among marine animals.

It has also been hypothesized that innovations in terrestrial evolution might have resulted in higher nutrient fluxes from land to sea. Specifically, Bambach [43] hypothesized that flowering plants would have increased nutrient fluxes to the oceans, beginning in the mid-Cretaceous Period; however, Boyce & Lee [88] subsequently showed that the timing of angiosperm radiation fits poorly with patterns of Mesozoic marine evolution. On the other hand, seagrass and mangrove communities would have provided nutrient-rich nurseries for coastal animals from the Late Cretaceous onwards [89,90].

Diatoms were not part of the earliest Mesozoic phytoplankton radiations, but beginning in the Cretaceous Period and accelerating into the Early Cenozoic Era, they diversified to become major primary producers in productive ocean waters. In light of the hypothesized increase in continental run-off and, thus, nutrient enrichment, the radiation of phytoplanktonic diatoms can be interpreted in terms of the models described above. Increasing primary production would have facilitated the evolution of larger phytoplankton cells, opening a niche for diatoms, perhaps especially at high latitude sites of strong upwelling [91]. Cermeño *et al.* [62] have, in fact, proposed that the dissolved silica levels needed to support high diatom production are themselves a product of increased continental weathering and erosion. Large diatom cells, in turn, would have shortened food chains, increasing the flux of energy to top predators. That is, by shortening food chains, diatoms may have amplified the ecosystem consequences of increasing primary production. Moreover, limited ecological experiments suggest that bivalves fed on diatom-rich diets grow faster than those fed on green algae [92,93], supporting the hypothesis that the carbon (C):N:P of diatoms (and coccolithophorids) promotes more efficient growth of grazers, again moving more energy upward through food webs [94,95].

In short, evolutionary changes in the composition of phytoplankton could have enabled much of the observed Mesozoic marine revolution among animals, whether or not net primary production changed through time. We note that coccolithophorids, the third component of the Mesozoic phytoplankton radiation, have not figured strongly in our perspective because their cells are neither large nor strongly mixotrophic. Coccolithophorids could, however, have contributed to Mesozoic ecosystem change to the extent that their mineralized scales served to facilitate export production, increasing remineralization depth and, through this, phosphate availability and, in consequence, primary production [96]. The radiations of both diatoms and coccolithophorids had signal biogeochemical consequences, not only increasing rates of organic matter export from surface water masses [96], but also changing the marine carbonate [97] and silica [98] cycles.

If radiating phytoplankton fuelled faunal change in Mesozoic oceans, what facilitated Mesozoic phytoplankton evolution? At present, this question has no definitive answer, but various lines of evidence hint at the right direction. Molecular clock estimates suggest that photosynthetic stramenopiles [99] and haptophytes [100] originated during the Neoproterozoic Era, long before the specific radiations of diatoms and coccolithophorids. Similarly, dinoflagellates appear to have Neoproterozoic origins, although whether early members of the clade were photosynthetic is less clear [101]. Such considerations suggest that Mesozoic phytoplankton radiations reflect specific innovations within already extant clades, environmental changes that favoured these clades, or both.

In one view end-Permian mass extinction facilitated the rise to ecological prominence of chlorophyll *a+c*-bearing phytoplankton [102,103], either through selective survival or via the establishment of favourable environmental conditions during Triassic recovery. As Medlin [103] observed, however, whatever the role of end-Permian extinction, the subsequent ecological expansion of dinoflagellates and coccolithophorids must be understood in terms of physiological characters that promoted competitive success in Mesozoic

oceans. Biomarker lipids document the continuing ecological importance of green algae through the Triassic Period [104].

Kooistra *et al.* [105] reviewed characters that underpin the ecological and evolutionary success of the diatoms, calling attention to pigments that capture a relatively broad and energetic portion of the visible light spectrum, highly efficient nutrient uptake, a vacuole capable of storing nitrate, and both physical (the siliceous frustule) and chemical defences against grazers. All may have played a role in the rise of the diatoms, but changing ocean chemistry and nutrient availability probably did as well. The case for increasing nutrient availability, beginning in the later Cretaceous Period and enhanced by long-term changes in ocean circulation and climate [60], has already been made, as has the corollary argument that increasing macronutrients would be accompanied by enhanced silica availability. Limited experiments support the view that diatom success reflects the interaction of biological innovation with environmental circumstance. For example, when Ratti *et al.* [106] ran competition experiments using selected diatoms, green algae, and cyanobacteria, the diatoms emerged as dominant in the present-day seawater, but were outcompeted by green algae in solutions designed to simulate seawater in mid-Paleozoic oceans.

Similarly resolved character analyses are not available for coccolithophorids and dinoflagellates, but they share a basic set of photosynthetic pigments with diatoms, and coccolithophorids, at least, share the presence of a biomineralized surface. Indeed, unlike animals, in which most innovations in skeletal biomineralization occurred in association with Cambrian diversification, planktonic protists show a Mesozoic peak in the first appearances of both siliceous and calcareous tests and scales [107]. This suggests increased Mesozoic predation pressure in parts of the food chain unassayed by Vermeij. It has also been observed that dinoflagellates, coccolithophorids, and diatoms have a lower iron (Fe) quotient than green algae and cyanobacteria, providing an advantage in increasingly well-oxygenated ocean basins [108], as well as enhanced growth at sulfate levels probably first sustained in Mesozoic oceans [106]. This issue deserves further study, especially as it is amenable to both experimentation (e.g. [106,109]) and exploration with suitable models [73,77,78,91].

References

- Vermeij GJ. 1977 The Mesozoic marine revolution: evidence from snails, predators and grazers. *Paleobiology* **3**, 245–258. (doi:10.1017/S0094837300005352)
- Vermeij GJ. 1987 *Evolution and escalation: an ecological history of life*. Princeton, NJ: Princeton University Press.
- Vermeij GJ. 2013 On escalation. *Annu. Rev. Earth Planet. Sci.* **41**, 1–19. (doi:10.1146/annurev-earth-050212-124123)
- Paytan A. 2009 Ocean paleoproductivity. In *Encyclopedia of paleoclimatology and ancient environments* (ed. V Goernitz), pp. 644–651. Dordrecht, The Netherlands: Springer.
- Allmon WD, Martin RE. 2014 Seafood through time revisited: the Phanerozoic increase in marine trophic resources and its macroevolutionary consequences. *Paleobiology* **40**, 255–286. (doi:10.1666/13065)
- Bambach RK. 1993 Seafood through time: changes in biomass, energetics, and productivity in the marine ecosystem. *Paleobiology* **19**, 372–397. (doi:10.1017/S0094837300000336)
- Holland SM, Sclafani JA. 2015 Phanerozoic diversity and neutral theory. *Paleobiology* **41**, 369–376. (doi:10.1017/pab.2015.10)
- Vermeij GJ. 1974 Marine faunal dominance and molluscan shell form. *Evolution* **28**, 656–674. (doi:10.2307/2407289)
- Vermeij GJ. 1976 Inter-oceanic differences in vulnerability of shelled prey to crab predation. *Nature* **260**, 135–136. (doi:10.1038/260135a0)
- Hughes RN, Elnor RW. 1979 Tactics of a predator, *Carcinus maenas*, and morphological responses of the prey, *Nucella lapillus*. *J. Anim. Ecol.* **48**, 65–78. (doi:10.2307/4100)
- Bertness MD, Cunningham C. 1981 Crab shell-crushing predation and gastropod architectural defense. *J. Exp. Mar. Biol. Ecol.* **50**, 213–230. (doi:10.1016/0022-0981(81)90051-4)
- Lowell RB. 1986 Crab predation on limpets: predator behavior and defensive features of the shell morphology. *Biol. Bull.* **171**, 577–596. (doi:10.2307/1541625)
- Preston SJ, Revie IC, Orr JF, Roberts D. 1996 A comparison of the strengths of gastropod shells with forces generated by potential crab predators. *J. Zool. Lond.* **238**, 181–193. (doi:10.1111/j.1469-7996.1996.tb05388.x)
- Kroger B. 2002 Antipredatory traits of the ammonoid shell – indications from Jurassic

6. Conclusion

Models originally articulated to explore phytoplankton ecology and biogeography in the present-day ocean provide a new perspective on ecosystem change in ancient oceans, supporting Vermeij's [1] proposal that top-down controls on Mesozoic marine evolution reflect bottom-up facilitation. The novelty of the viewpoint presented here lies in the argument that changes in the *composition* of Mesozoic primary producer communities, and not simply the *amount* of primary production, fuelled observed faunal changes documented by Mesozoic and early Cenozoic fossils. A combination of mechanisms may have enhanced and accelerated the flux of resources through primary producers to the trophic levels where the arms race chronicled by Vermeij took place. At the outset, a marked radiation of mixotrophic dinoflagellates may have accelerated the transfer of primary production upward into larger size classes and higher trophic levels. Then, nutrient enhancement by increased global rates of continental run-off likely boosted ocean productivity, enhancing productivity in larger size classes, and opening up ecological opportunities for diatom radiation. The high maximum growth rates of phytoplanktonic diatoms further accelerated the productivity of larger size classes, again promoting the flow of fixed carbon to higher trophic levels.

Thus, a combination of biogeochemical and evolutionary events conspired to make more resources available to middle trophic levels of the marine ecosystem, providing impetus for the Mesozoic marine revolution and its associated arms race. This perspective underscores the utility of considering palaeontological patterns of animal evolution within a broader ecological framework and indicates that ecosystem modelling can improve our understanding of the marine biota in time as well as in space.

Authors' contributions. A.H.K. conceived the study; M.J.F. constructed the models; and both authors contributed to the writing of this paper.

Competing interests. We have no competing interests.

Funding. A.H.K.'s research was funded by a grant from the Keck Foundation. M.J.F.'s research was funded by the Gordon and Betty Moore Foundation (GBMF no. 3778).

- ammonoids with sublethal injuries. *Paläontol. Z.* **77**, 223–234. (doi:10.1007/BF02989859)
15. Kerr JP, Kelley PH. 2015 Assessing the influence of escalation during the Mesozoic marine revolution: shell breakage and adaptation against enemies in Mesozoic ammonites. *Palaeogeogr. Palaeoclimatol. Palaeoecol.* **440**, 632–646. (doi:10.1016/j.palaeo.2015.08.047)
 16. Molinaro DJ, Stafford ES, Collins BMJ, Barclay KM, Tyler CL, Leighton LR. 2014 Peeling out predation intensity in the fossil record: a test of repair scar frequency as a suitable proxy for predation pressure along a modern predation gradient. *Palaeogeogr. Palaeoclimatol. Palaeoecol.* **412**, 141–147. (doi:10.1016/j.palaeo.2014.07.033)
 17. McRoberts CA. 2001 Triassic bivalves and the initial marine Mesozoic revolution: a role for predators? *Geology* **29**, 359–362. (doi:10.1130/0091-7613(2001)029<0359:TBATIM>2.0.CO;2)
 18. Stanley SM. 1977 Trends, rates, and patterns of evolution in the Bivalvia. In *Patterns of evolution, as illustrated by the fossil record* (ed. A Hallam), pp. 209–250. Amsterdam, The Netherlands: Elsevier.
 19. Leonard-Pingel JS, Jackson JBC. 2013 Drilling intensity varies among Neogene tropical American Bivalvia in relation to shell form and life habit. *Bull. Mar. Sci.* **89**, 905–919. (doi:10.5343/bms.2012.1058)
 20. Stanley SM. 1968 Post-Paleozoic adaptive radiation of infaunal bivalve molluscs: a consequence of mantle fusion and siphon formation. *J. Paleontol.* **42**, 14–29.
 21. Aberhan M, Kiessling W, Fürsich FT. 2006 Testing the role of biological interactions in the evolution of mid-Mesozoic marine benthic ecosystems. *Paleobiology* **32**, 259–277. (doi:10.1666/05028.1)
 22. Mondal S, Harries PJ. 2016 Phanerozoic trends in ecospace utilization: the bivalve perspective. *Earth-Sci. Rev.* **152**, 106–118. (doi:10.1016/j.earscirev.2015.10.005)
 23. Oji T. 1996 Is predation intensity reduced with increasing depth? Evidence from the west Atlantic stalked crinoid *Endoxocrinus parrae* (Gervais) and implications for the Mesozoic marine revolution. *Paleobiology* **22**, 339–351. (doi:10.1017/S0094837300016328)
 24. Baumiller T, Salamon M, Gorzelak P, Mooi R, Messing C, Gahn F. 2010 Post-Paleozoic crinoid radiation in response to benthic predation preceded the Mesozoic marine revolution. *Proc. Natl Acad. Sci. USA* **107**, 5893–5896. (doi:10.1073/pnas.0914199107)
 25. Gorzelak P, Salamon MA, Baumiller TZ. 2010 Predator-induced macroevolutionary trends in Mesozoic crinoids. *Proc. Natl Acad. Sci. USA* **109**, 7004–7007. (doi:10.1073/pnas.1201573109)
 26. Aronson RB. 1989 A community-level test of the Mesozoic marine revolution theory. *Paleobiology* **15**, 20–25. (doi:10.1017/S0094837300009155)
 27. Aronson RB. 1991 Predation, physical disturbance, and sublethal arm damage in ophiuroids: a Jurassic-Recent comparison. *Mar. Ecol. Progr. Ser.* **74**, 91–97. (doi:10.3354/meps074091)
 28. Hopkins MJ, Smith AB. 2015 Dynamic evolutionary change in post-Paleozoic echinoids and the importance of scale when interpreting changes in rates of evolution. *Proc. Natl Acad. Sci. USA* **112**, 3758–3763. (doi:10.1073/pnas.1418531112)
 29. Vörös A. 2010 Escalation reflected in the ornamentation and diversity history of brachiopod clades during the Mesozoic marine revolution. *Palaeogeogr. Palaeoclimatol. Palaeoecol.* **291**, 474–480. (doi:10.1016/j.palaeo.2010.03.018)
 30. Ruban DA. 2011 Diversity dynamics of Callovian-Albian brachiopods in the northern Caucasus (northern Neo-Tethys) and a Jurassic/Cretaceous mass extinction. *Paleontol. Res.* **15**, 154–167. (doi:10.2517/1342-8144-15.3.154)
 31. Steneck RS. 1983 Escalating herbivory and resulting adaptive trends in calcareous algal crusts. *Paleobiology* **9**, 44–61. (doi:10.1017/S0094837300007375)
 32. Madin JS, Alroy J, Aberhan M, Fürsich FT, Kiessling W, Kosnik MA, Wagner PJ. 2006 Statistical independence of escalatory ecological trends in Phanerozoic marine invertebrates. *Science* **312**, 897–900. (doi:10.1126/science.1123591)
 33. Roopmarine PD, Angielczyk KD, Hertog R. 2006 Comment on ‘Statistical independence of escalatory ecological trends in Phanerozoic marine invertebrates’. *Science* **314**, p925d. (doi:10.1126/science.1130073)
 34. Dietl GP, Vermeij GJ. 2006 Comment on ‘Statistical independence of escalatory ecological trends in Phanerozoic marine invertebrates’. *Science* **314**, p925e. (doi:10.1126/science.1130419)
 35. Vermeij GJ. 2008 Escalation and its role in Jurassic biotic history. *Palaeogeogr. Palaeoclimatol. Palaeoecol.* **263**, 3–8. (doi:10.1016/j.palaeo.2008.01.023)
 36. Madin JS, Alroy J, Aberhan M, Fürsich FT, Kiessling W, Kosnik MA, Wagner PJ. 2006 Response to comments on ‘Statistical independence of escalatory ecological trends in Phanerozoic marine invertebrates’. *Science* **314**, 925f. (doi:10.1126/science.1131363)
 37. Stanley SM. 1974 What has happened to the articulate brachiopods? *Geol. Soc. Am. Abstr. Progr.* **6**, 966–967.
 38. Signor PW, Brett CE. 1984 The mid-Paleozoic precursor to the Mesozoic marine revolution. *Paleobiology* **10**, 229–245. (doi:10.1017/S0094837300008174)
 39. Kelley NP, Pyenson ND. 2015 Evolutionary innovation and ecology in marine tetrapods from the Triassic to the Anthropocene. *Science* **384**, aaa3716. (doi:10.1126/science.aaa3716)
 40. Schweitzer CM, Feldmann RM. 2010 The Decapoda (Crustacea) as predators on Mollusca through geologic time. *Palaio* **25**, 167–182. (doi:10.2110/palo.2009.p09-054r)
 41. Harper EM. 2006 Dissecting post-Paleozoic arms races. *Palaeogeogr. Palaeoclimatol. Palaeoecol.* **232**, 322–343. (doi:10.1016/j.palaeo.2005.05.017)
 42. Donovan TSK, Gale AS. 1990 Predatory asteroids and the decline of the articulate brachiopods. *Lethaia* **23**, 77–86. (doi:10.1111/j.1502-3931.1990.tb01782.x)
 43. Bambach RK. 1999 Energetics in the global marine fauna: a connection between terrestrial diversification and change in the marine biosphere. *Geobios* **32**, 131–144. (doi:10.1016/S0016-6995(99)80025-4)
 44. Bush AM, Bambach RK. 2011 Paleoeological megatrends in marine metazoa. *Annu. Rev. Earth Planet. Sci.* **39**, 241–269. (doi:10.1146/annurev-earth-040809-152556)
 45. Huntley JW, Kowalewski M. 2007 Coupling of predation intensity and diversity in the Phanerozoic fossil record. *Proc. Natl Acad. Sci. USA* **104**, 15 006–15 010. (doi:10.1073/pnas.0704960104)
 46. Oji T, Ogaya C, Sato T. 2003 Increase of shell-crushing predation recorded in fossil shell fragmentation. *Paleobiology* **29**, 520–529. (doi:10.1666/0094-8373(2003)029<0520:IOSPRI>2.0.CO;2)
 47. de Vargas C *et al.* 2015 Eukaryotic plankton diversity in the sunlit ocean. *Science* **348**, 1261605. (doi:10.1126/science.1261605)
 48. Falkowski PG, Katz ME, Knoll AH, Quigg A, Raven JA, Schofield O, Taylor FJR. 2004 The evolution of modern eukaryotic phytoplankton. *Science* **305**, 354–360. (doi:10.1126/science.1095964)
 49. Spencer-Cervato C. 1999 The Cenozoic deep sea microfossil record: explorations of the DSDP/ODP sample set using the Neptune database. *Palaeontolog. Electronica* **2**, 4. See http://palaeo-electronica.org/1999_2/neptune/issue2_99.htm.
 50. Bown PR, Lees JA, Young JR. 2004 Calcareous nannoplankton evolution and diversity through time. In *Coccolithophores: from molecular processes to global impact* (eds H Thierstein, JR Young), pp. 481–505. Amsterdam, The Netherlands: Elsevier.
 51. Stover LE *et al.* 1996 Mesozoic-Tertiary dinoflagellates, acritarchs and prasinophytes. In *Palyinology: principles and applications*, vol. 2 (eds J Jansonius, DC McGregor), pp. 641–750. Dallas, TX: American Association of Stratigraphic Palynologists Foundation.
 52. Hammer AC, Pitchford JW. 2005 The role of mixotrophy in plankton bloom dynamics, and the consequences for productivity. *ICES J. Mar. Sci.* **62**, 833–840. (doi:10.1016/j.icesjms.2005.03.001)
 53. Holba AG, Tegelaar EW, Huizinga BJ, Moldovan JM, Singletary MS, McCaffrey MA, Dzou LIP. 1998 24-norcholestanes as age-sensitive molecular fossils. *Geology* **26**, 783–786. (doi:10.1130/0091-7613(1998)026<0783:NAASMF>2.3.CO;2)
 54. Sinninghe Damste JS *et al.* 2004 The rise of the rhizolenid diatoms. *Science* **304**, 584–587. (doi:10.1126/science.1096806)
 55. Knoll AH, Summons RE, Waldbauer J, Zumberge J. 2007 The geological succession of primary producers in the oceans. In *The evolution of primary producers in the sea* (eds P Falkowski, AH Knoll), pp. 133–163. Burlington, MA: Elsevier.
 56. John U, Fensome RA, Medlin LK. 2003 The application of a molecular clock based on molecular sequences and the fossil record to explain biogeographic distributions within the *Alexandrium*

- tamarensis* 'species complex' (Dinophyceae). *Mol. Biol. Evol.* **20**, 1015–1027. (doi:10.1093/molbev/msg105)
57. Sorhannus U. 2007 A nuclear-encoded small-subunit ribosomal RNA timescale for diatom evolution. *Mar. Micropaleontol.* **65**, 1–12. (doi:10.1016/j.marmicro.2007.05.002)
58. Medlin LK, Fensome RA. 2013 Dinoflagellate macroevolution: some considerations based on an integration of molecular, morphological and fossil evidence. In *Biological and geological perspectives of dinoflagellates* (eds JM Lewis, F Marret, L Bradley), pp. 263–274. Micropaleontological Society, Special Publications. London, UK: Geological Society.
59. Medlin LK, Sáez AG, Young JR. 2008 A molecular clock for coccolithophores and implications for selectivity of phytoplankton extinctions at the K/T boundary. *Mar. Micropaleontol.* **67**, 69–86. (doi:10.1016/j.marmicro.2007.08.007)
60. Katz ME, Finkel ZV, Grzebyk D, Falkowski PG, Knoll AH. 2004 Evolutionary trajectories and biogeochemical impacts of marine eukaryotic phytoplankton. *Annu. Rev. Ecol. Systemat.* **35**, 523–556. (doi:10.1146/annurev.ecolsys.35.112202.130137)
61. Rabosky DL, Sorhannus U. 2009 Diversity dynamics of marine planktonic diatoms across the Cenozoic. *Nature* **457**, 183–186. (doi:10.1038/nature07435)
62. Cermeno P, Falkowski PG, Romero OE, Schaller MF, Vallina SM. 2015 Continental erosion and the Cenozoic rise of marine diatoms. *Proc. Natl Acad. Sci. USA* **112**, 4239–4244. (doi:10.1073/pnas.1412883112)
63. Kotrc B, Knoll AH. 2015 A morphospace of planktonic marine diatoms. I. Two views of disparity through time. *Paleobiology* **41**, 45–67. (doi:10.1017/pab.2014.4)
64. Berman-Frank I, Lundgren P, Falkowski P. 2003 Nitrogen fixation and photosynthetic oxygen evolution in cyanobacteria. *Res. Microbiol.* **154**, 157–164. (doi:10.1016/S0923-2508(03)00029-9)
65. Grosskopf T, LaRoche J. 2012 Direct and indirect costs of dinitrogen fixation in *Crocospaera watsonii* WH8501 and possible implications for the nitrogen cycle. *Front. Microbiol.* **3**, 236. (doi:10.3389/fmicb.2012.00236)
66. Berman-Frank I, Lundgren P, Chen Y-B, Küpper H, Kolber Z, Bergman B, Falkowski P. 2001 Segregation of nitrogen fixation and oxygenic photosynthesis in the marine cyanobacterium *Trichodesmium*. *Science* **294**, 1534–1537. (doi:10.1126/science.1064082)
67. Ward BA, Dutkiewicz S, Moore CM, Follows MJ. 2013 Iron, phosphorus, and nitrogen supply ratios define the biogeography of nitrogen fixation. *Limnol. Oceanogr.* **58**, 2059–2075. (doi:10.4319/lo.2013.58.6.2059)
68. Stewart FM, Levin BR. 1973 Partitioning of resources and the outcome of interspecific competition: a model and some general considerations. *Am. Nat.* **107**, 171–198. (doi:10.1086/282825)
69. Tilman D. 1977 Resource competition between plankton algae: an experimental and theoretical approach. *Ecology* **58**, 338–348. (doi:10.2307/1935608)
70. Edwards KF, Thomas MK, Klausmeier CA, Litchman E. 2012 Allometric scaling and taxonomic variation in nutrient utilization traits and maximum growth rate of phytoplankton. *Limnol. Oceanogr.* **57**, 554–566. (doi:10.4319/lo.2012.57.2.0554)
71. Armstrong RA. 1994 Grazing limitation and nutrient limitation in marine ecosystems: steady state solutions of an ecosystem model with multiple food chains. *Limnol. Oceanogr.* **39**, 597–608. (doi:10.4319/lo.1994.39.3.0597)
72. Poulin FJ, Franks PJS. 2010 Size-structured planktonic ecosystems: constraints, controls and assembly instructions. *J. Plankton Res.* **32**, 1121–1130. (doi:10.1093/plankt/fbp145)
73. Ward BA, Dutkiewicz S, Follows MJ. 2014 Modelling spatial and temporal patterns in size-structured marine plankton communities: top-down and bottom-up controls. *J. Plankton Res.* **36**, 31–47. (doi:10.1093/plankt/fbt097)
74. Hansen PJ, Bjørnsen PK, Hansen BW. 1997 Zooplankton grazing and growth: scaling with the 2–2000 mm body size range. *Limnol. Oceanogr.* **42**, 678–704. (doi:10.4319/lo.1997.42.4.0687)
75. Chisholm SW. 1992 Phytoplankton size. In *Primary productivity and biogeochemical cycles in the sea* (eds PG Falkowski, AD Woodhead), pp. 213–237. New York, NY: Plenum Press.
76. Sheldon RW, Prakash A, Sutcliffe WHJ. 1972 The size distribution of particles in the ocean. *Limnol. Oceanogr.* **17**, 327–340. (doi:10.4319/lo.1972.17.3.0327)
77. Litchman E, Klausmeier CA, Schofield OM, Falkowski PG. 2007 The role of functional traits and trade-offs in structuring phytoplankton communities: scaling from cellular to ecosystem level. *Ecol. Lett.* **10**, 1170–1181. (doi:10.1111/j.1461-0248.2007.01117.x)
78. Ward BA, Follows MJ. 2016 Marine mixotrophy increases trophic transfer efficiency, mean organism size and vertical carbon flux. *Proc. Natl Acad. Sci. USA* **113**, 2958–2963. (doi:10.1073/pnas.1517118113)
79. Raven JA, Waite AM. 2004 The evolution of silicification in diatoms: inescapable sinking and sinking as escape? *New Phytol.* **162**, 45–61. (doi:10.1111/j.1469-8137.2004.01022.x)
80. Paytan A, Griffith EM. 2007 Marine barite: recorder of variations in ocean export productivity. *Deep-Sea Res. II. Top. Stud. Oceanogr.* **54**, 687–705. (doi:10.1016/j.dsr2.2007.01.007)
81. Veizer J *et al.* 1999 $^{87}\text{Sr}/^{86}\text{Sr}$, $\delta^{13}\text{C}$ and $\delta^{18}\text{O}$ evolution of Phanerozoic seawater. *Chem. Geol.* **161**, 59–88. (doi:10.1016/S0009-2541(99)00081-9)
82. Derry LA, France-Lanord C. 1996 Neogene Himalayan weathering history and river $^{87}\text{Sr}/^{86}\text{Sr}$: Impact on the marine Sr record. *Earth Planet. Sci. Lett.* **142**, 59–74. (doi:10.1016/0012-821X(96)00091-X)
83. Molnar P. 2004 Late Cenozoic increase in accumulation rates of terrestrial sediment: how might climate change have affected erosion rates? *Annu. Rev. Earth Planet. Sci.* **32**, 67–89. (doi:10.1146/annurev.earth.32.091003.143456)
84. Herman F, Seward D, Valla PG, Carter A, Kohn B, Willet SD, Ehlers TA. 2013 Worldwide acceleration of mountain erosion under a cooling climate. *Nature* **504**, 423–426. (doi:10.1038/nature12877)
85. Misra S, Froelich PN. 2012 Lithium isotope history of Cenozoic seawater: changes in silicate weathering and reverse weathering. *Science* **335**, 818–823. (doi:10.1126/science.1214697)
86. Willenbring JK, Jerolmack DJ. 2016 The null hypothesis: globally steady rates of erosion, weathering fluxes and shelf sediment accumulation during Late Cenozoic mountain uplift and glaciation. *Terre Nova* **28**, 11–18. (doi:10.1111/ter.12185)
87. Lechler M, Philip AE, van Strandmann P, Jenkyns HC, Prosser G, Pacente M. 2015 Lithium-isotope evidence for enhanced silicate weathering during OAE1a (Early Aptian Selli event). *Earth Planet. Sci. Lett.* **432**, 210–222. (doi:10.1016/j.epsl.2015.09.052)
88. Boyce CK, Lee J-E. 2011 Could land plant evolution have fed the marine revolution? *Paleontol. Res.* **15**, 100–105. (doi:10.2517/1342-8144-15.2.100)
89. Eva AN. 1980 Pre-Miocene seagrass communities in the Caribbean. *Palaeontology* **23**, 231–236.
90. Ellison AM, Farnsworth EJ, Merkt RE. 1999 Origins of mangrove ecosystems and the mangrove biodiversity anomaly. *Glob. Ecol. Biogeogr.* **8**, 95–115. (doi:10.1046/j.1466-822X.1999.00126.x)
91. Ward BA, Dutkiewicz S, Jahn O, Follows MJ. 2012 A size-structured food-web model for the global ocean. *Limnol. Oceanogr.* **57**, 1877–1891. (doi:10.4319/lo.2012.57.6.1877)
92. Epifanio CE. 1979 Growth in bivalve molluscs: nutritional effects of two or more species of algae in diets fed to the American Oyster *Crassostrea virginica* (Gmelin) and the hard clam *Mercenaria mercenaria* (L.). *Aquaculture* **18**, 1–12. (doi:10.1016/0044-8486(79)90095-4)
93. Enright CT, Newkirk GF, Craigie JS, Castell JD. 1981 Evaluation of phytoplankton as diets for juvenile *Ostrea edulis* L. *J. Exp. Mar. Biol. Ecol.* **96**, 1–13. (doi:10.1016/0022-0981(86)90009-2)
94. Martin R, Quigg A. 2012 Evolving phytoplankton stoichiometry fueled diversification of the marine biosphere. *Geosciences* **2**, 130–146. (doi:10.3390/geosciences2020130)
95. Sterner RW, Elser JJ. 2002 *Ecological stoichiometry: the biology of elements from molecules to the biosphere*. Princeton, NJ: Princeton University Press.
96. Meyer KA, Ridgwell A, Payne JL. 2016 The influence of the biological pump on ocean chemistry: implications for long-term trends in marine redox chemistry, the global carbon cycle, and marine animal ecosystems. *Geobiology* **14**, 207–219. (doi:10.1111/gbi.12176)
97. Milliman JD, Mueller G, Foerstner U. 1974 *Marine carbonates I: recent sedimentary carbonates*. New York, NY: Springer.
98. Maliva R, Knoll AH, Siever R. 1989 Secular change in chert distribution: a reflection of evolving biological participation in the silica cycle. *Palaia* **4**, 519–532. (doi:10.2307/3514743)

99. Brown JW, Sorhannus U. 2010 A molecular genetic timescale for the diversification of autotrophic stramenopiles (Ochromyza): substantive underestimation of putative fossil ages. *PLoS ONE* **5**, e12759. (doi:10.1371/journal.pone.0012759)
100. Young JN, Rickaby REM, Kaprolov MV, Filatov DA. 2012 Adaptive signals in algal Rubisco reveal a history of ancient atmospheric carbon dioxide. *Phil. Trans. R. Soc. B* **67**, 483–492. (doi:10.1098/rstb.2011.0145)
101. Delwiche CF. 2007 The origin and evolution of dinoflagellates. In *The evolution of primary producers in the sea* (eds P Falkowski, AH Knoll), pp. 191–205. Burlington, MA: Elsevier.
102. Payne JL, van de Schootbrugge B. 2007 Life in Triassic oceans: links between planktonic and benthic recovery and radiation. In *The evolution of primary producers in the sea* (eds P Falkowski, AH Knoll), pp. 165–189. Burlington, MA: Elsevier.
103. Medlin LK. 2011 The Permian–Triassic mass extinction forces the radiation of the modern marine phytoplankton. *Phycologia* **50**, 684–693. (doi:10.2216/10-31.1)
104. Saito R, Kaiho K, Oba M, Tong JN, Chen ZQ, Takahashi S, Chen J, Tian L, Biswas RK. 2016 Secular changes in environmental stresses and eukaryotes during the Early Triassic to the early Middle Triassic. *Palaeogeogr. Palaeoclimatol. Palaeoecol.* **451**, 35–45. (doi:10.1016/j.palaeo.2016.03.006)
105. Kooistra WHCF *et al.* 2007 The origin and evolution of the diatoms: their adaptation to a planktonic existence. In *The evolution of primary producers in the sea* (eds P Falkowski, AH Knoll), pp. 207–249. Burlington, MA: Elsevier.
106. Ratti S, Knoll AH, Giordano M. 2011 Did sulfate availability facilitate the evolutionary expansion of chlorophyll a+c phytoplankton in the oceans? *Geobiology* **9**, 301–312. (doi:10.1111/j.1472-4669.2011.00284.x)
107. Knoll AH, Kotrc B. 2015 Protistan skeletons: a geologic history of evolution and constraint. In *Evolution of lightweight structures* (ed. C Hamm), pp. 3–16. Berlin, Germany: Springer.
108. Quigg A, Finkel ZV, Irwin AJ, Rosenthal Y, Ho TY, Reinfelder JR, Schofield O, Morel FMM, Falkowski PG. 2003 The evolutionary inheritance of elemental stoichiometry in marine phytoplankton. *Nature* **425**, 291–294. (doi:10.1038/nature01953)
109. Ratti S, Knoll AH, Giordano M. 2013 Grazers and phytoplankton growth in the oceans: an experimental and evolutionary perspective. *PLoS ONE* **8**, e77349. (doi:10.1371/journal.pone.0077349)